The Astrophysical Journal, 589:481–486, 2003 May 20

NEUTRINOS FROM ACCRETING NEUTRON STARS

Luis A. Anchordoqui,[1] Diego F. Torres,[2] Thomas P. McCauley,[1] Gustavo E. Romero,[3] and Felix A. Aharonian[4]

Received 2002 November 20; accepted 2003 January 29

ABSTRACT

The magnetospheres of accreting neutron stars develop electrostatic gaps with huge potential drops. Protons and ions, accelerated in these gaps along the dipolar magnetic field lines to energies greater than 100 TeV, can impact onto the surrounding accretion disk. A proton-induced cascade develops, and charged pion decays produce ν emission. With extensive disk shower simulations using DPMJET and GEANT4, we have calculated the resulting ν spectrum. We show that the spectrum produced out of the proton beam is a power law. We use this result to propose accretion-powered X-ray binaries (with highly magnetized neutron stars) as a new population of pointlike ν sources for kilometer-scale detectors such as ICECUBE. As a particular example, we discuss the case of A0535+26. We show that ICECUBE should find A0535+26 to be a periodic ν source, one for which the formation and loss of its accretion disk can be fully detected. Finally, we comment briefly on the possibility that smaller telescopes such as AMANDA could also detect A0535+26 by folding observations with the orbital period.

Subject headings: gamma rays: observations — gamma rays: theory — neutrinos — X-rays: binaries — X-rays: individual (A0535+26)

1. INTRODUCTION

X-ray binaries have fascinated those looking for Galactic neutrino sources (Berezinsky, Castagnoli, & Galeotti 1985; Kolb, Turner, & Walker 1985; Gaisser & Stanev 1985). The basic idea is to somehow use the secondary object in the system to accelerate protons, which then could collide within a higher density medium. One possibility that was earlier explored was to use the primary itself as the target for those accelerated hadrons (Berezinsky et al. 1990). Depending on the grazing angle of the colliding protons, on the size and type of the primary star, and on the effectiveness of the acceleration mechanism, γ-rays and neutrinos (or ν's) could escape from the system. Gamma rays, however, could more naturally be produced in the accretion disk surrounding the neutron stars: detailed models for this possibility were presented by Cheng & Ruderman (1989). Here we show that accreting X-ray binaries in which the compact object is a magnetized neutron star are sources of high-energy neutrinos that can be detected by forthcoming neutrino telescopes. Moreover, we show that the signal-to-noise ratio (S/N) can be high enough as to allow timing studies and multiwavelength comparison.

2. THE ACCRETION DISK OF A0535+26

Of all the X-ray binaries, A0535+26 is one of the most studied. A0535+26 is a Be-/X-ray transient in which the compact object is a 104 s pulsar in an eccentric orbit around the B0 III star HDE 245770. Be stars are rapidly rotating objects that eject mass, irregularly forming gaseous disks in their equatorial planes. Strong and recurrent X-ray outbursts were observed separated by 111 days, which has been identified with the orbital period (Giovannelli & Sabau Graziati 1992). These outbursts occur when the accretion onto the neutron star increases at periastron passage. (The average ratio of the X-ray luminosity at the periastron to that of apoastron is ~100; Janot-Pacheco, Motch, & Mouchet 1987.) The BATSE instrument of the *Compton Gamma Ray Observatory* detected a 33 day, broad, quasi-periodic oscillation in the power spectra of the X-ray flux, definitively showing that an accretion disk is formed during giant outbursts (Finger, Wilson, & Harmon 1996). The γ-ray light-curve maximum for this object is anticorrelated with X-rays at periastron passage (Hartman et al. 1999; Romero et al. 2001). To explain this anticorrelation, a variation in the disk grammage is invoked: when the disk is fully formed and the X-ray luminosity is at its maximum, the disk grammage is too high to allow γ-ray photons above 100 MeV to escape. We now describe how the accretion disk model works.

Accretion disks can penetrate the stellar magnetospheres of accreting rotating neutron stars (Ghosh & Lamb 1979a). This penetration creates a broad transition zone between the unperturbed disk flow—far from the star—and the corotating magnetospheric flow—close to the star. In the transition zone, with inner radius r_0, the angular velocity is Keplerian. Between r_0 and the corotation radius r_{co}, there is a thin boundary layer where the angular velocity significantly departs from the Keplerian value. At r_{co}, the disk is disrupted by the magnetic pressure, and the accreting mass is channeled by the field to impact onto the stellar surface, producing strong X-ray emission.

The magnetosphere of an accreting neutron star spinning slower than that of the accretion disk can be divided into three regions as follows: (1) a region coupled to the star by the magnetic field lines that do not penetrate the disk, (2) an equatorial region linked to the disk by the field attached to it, and (3) a gap entirely empty of plasma separating both regions (Cheng & Ruderman 1989). The magnetospheric region penetrated by field lines that do not intersect the disk

[1] Department of Physics, Northeastern University, 110 Forsyth Street, Boston, MA 02115; doqui@neu.edu.

[2] Lawrence Livermore National Laboratory, 7000 East Avenue, L-413, Livermore, CA 94550; dtorres@igpp.ucllnl.org.

[3] Instituto Argentino de Radioastronomía (IAR), C.C. 5, 1894 Villa Elisa, Argentina.

[4] Max-Planck-Institut für Kernphysik, Posfach 10 39 80, D-69029 Heidelberg, Germany.

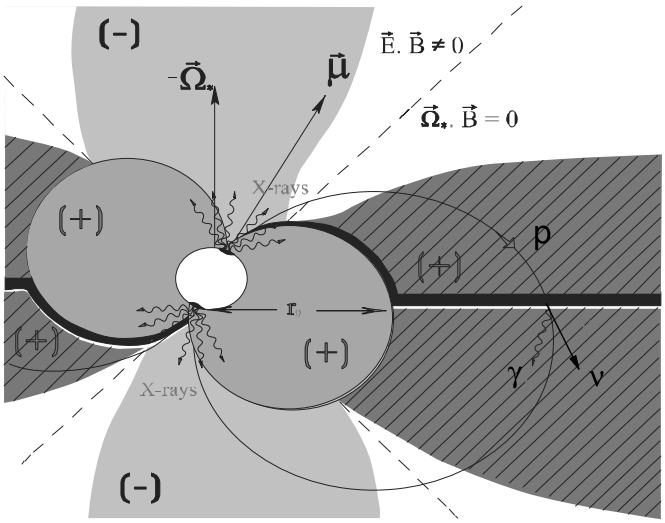

FIG. 1.—Sketch (not to scale) of the magnetosphere of an accreting magnetized neutron star, with the electrostatic gap produced when $\Omega_* < \Omega_d$. Protons entering into the gap from the region that corotates with the star (−) are accelerated along the field lines and impact onto the disk, initiating a shower; ν's and γ-ray photons, resulting from pion decay, emerge from the opposite side of the disk and will generically be beamed due to momentum conservation. This figure is adapted from several of the works by Cheng & Ruderman quoted in the text.

corotates with the star at an angular velocity Ω_*. When the angular velocity of the disk Ω_d exceeds the angular velocity of the star ($\Omega_* < \Omega_d$), the equatorial plasma between the inner accretion disk radius r_0 and the Alfvén radius r_A corotates with the disk to which it is linked by the frozen field lines. Inertial effects result in a charge separation around the null surface, $\boldsymbol{\Omega}_* \times \boldsymbol{B} = 0$. This leads to the formation of an electrostatic gap with no charge (see Fig. 1). In this gap, $\boldsymbol{E} \times \boldsymbol{B} \neq 0$, and a strong potential drop is established. The maximum potential drop along the magnetic field lines through the gap is (Cheng & Ruderman 1989)

$$V_{\max} \sim 4 \times 10^{14} \beta^{-5/2} \left(\frac{M_*}{M_\odot}\right)^{1/7} R_6^{-4/7} L_{37}^{5/7} B_{12}^{-3/7} \ V \ , \quad (1)$$

where $M_* \sim 1.4$–$2.7 \ M_\odot$ is the neutron star mass (Giovannelli & Sabau Graziati 1992), $R_6 \equiv R_*/10^6$ cm is its radius, $B_{12} \equiv B_*/10^{12}$ G is the magnetic field of the star, L_{37} is the X-ray luminosity in units of 10^{37} ergs s^{-1}, and $\beta \equiv 2r_0/r_A$ is twice the ratio between the inner accretion disk radius and the Alfvén radius. The Alfvén radius for spherical accretion can be determined from the condition that the unscreened magnetic energy density of the stellar field becomes comparable to the kinetic energy density of the accreting matter (Cheng & Ruderman 1989),

$$r_A \approx 3 \times 10^8 \ L_{37}^{-2/7} \ B_{12}^{4/7} \left(\frac{M_*}{M_\odot}\right)^{1/7} R_6^{10/7} \text{cm} \ . \quad (2)$$

The electrostatic gap hovers on the accretion disk from the innermost disk radius, $\sim r_0$ up to a distance of about r_A. Without loss of generality, we can assume that the stellar magnetic dipolar moment ($\mu = B_* R_*^3/2$) that induces B field lines across the disk is aligned with the rotation axis of the system (Cheng & Ruderman 1991). The B field on the disk, however, strongly depends on the screening factor generated by currents induced in the disk surface. In what follows, we take a mean B field of 6000 G (Ghosh & Lamb 1979b).

Protons entering into the gap from the stellar corotating region are accelerated up to energies $eV_{\max}$ and directed to the accretion disk by the field lines. The maximum current that can flow through the gap can be determined from the requirement that the azimuthal magnetic field induced by the current does not exceed that of the initial magnetic field (Cheng & Ruderman 1989),

$$J_{\max} \sim 1.5 \times 10^{24} \beta^{-2} \left(\frac{M_*}{M_\odot}\right)^{-2/7} R_6^{1/7} L_{37}^{4/7} B_{12}^{-1/7} \text{ esu s}^{-1} \ . \quad (3)$$

The mean number of protons impacting the disk is huge, $N_p = J_{\max}/e \sim 10^{33}$ s^{-1}, and the total power deposited by the proton beam in the disk is $P_{\max} = J_{\max} V_{\max} \sim 10^{36}$ ergs s^{-1}. The collision of the relativistic proton beam with the disk initiates hadronic and electromagnetic showers in which high-energy ν's are produced from the decay of charged pions, whereas γ-rays are produced from the decay of their neutral partners.

3. PHENOMENOLOGY

The system just described is an ideal source of high-energy ν's: it has a very dense material for pp-interactions and, at the same time, the region of acceleration is separated from that of high density, where interactions occur. The high-energy ν production in accretion disks of neutron stars is, however, subject to very stringent conditions on the disk grammage. The latter should be large enough to allow protons to interact and small enough to allow pions to decay or to escape so as to avoid losing energy. But the disk grammage is actually a periodically varying function in these systems, which follows the orbital dynamics. As noted, this fact was used to explain why the X-ray maximum is coincident with a nondetection in the γ-ray band for the system A0535+26 (Romero et al. 2001). An examination of the cross sections involved is in order.

In the energy range of interest, the $p\pi$ cross section, $\sigma_{p\pi} \sim 25$ mb (Carroll et al. 1979), is not too far away from the cross section for γ-ray absorption in the Coulomb field produced by disk ions, $\sigma_{\gamma E} \sim 10$ mb (Cox et al. 2001; Bethe & Heitler 1934). Then photons with energies more than 100 MeV undergo interactions within typical accretion disks if the mean density of hydrogen is $n \gtrsim 1 \times 10^{20}$ cm^{-3}. (The survival probability for γ-rays to a distance comparable to the thickness of the disk due to this process is less than 0.1%.) Moreover, assuming a source luminosity $L_{37} \sim 1$ in the form of $\approx$1 keV photons and an average disk radius of $\bar{r} \approx 2 \times 10^8$ cm, the energy density inside the disk is roughly $L_{37}/(2\pi \bar{r}^2 \ c) \simeq 10^9$ ergs cm^{-3}, implying a number density of 1 keV photons $\sim 10^{18}$ cm^{-3}.

Therefore, the secondary electrons and γ-rays most effectively interact with the radiation field of the disk. These secondary electrons originating from decays of neutral and charged π mesons will trigger an electromagnetic cascade in this field, resulting in a standard cascade spectrum with a cutoff energy around $m_e^2 c^4/\epsilon \approx 250 \ (\epsilon/1 \text{ keV})^{-1}$ MeV, where m_e is the mass of the electron and ϵ is the average energy of the background thermal photons.

According to canonical accretion disk models, the average density scales as $n \propto L_{37}^{20/35} \ (M_*/M_\odot)^{-1/28} \ r^{-21/20}$ (Shapiro & Teukolsky 1983). We normalize the particle

density of the accretion disk at $\bar{r}$ in order to fit γ-ray observations of A0535+26 (strong photon absorption in the periastron of the system, where $L_{37} \approx 1$; Finger et al. 1996). Because of the similarity in the cross sections discussed above, whenever γ-rays are absorbed, there will be a much-reduced signal in ν's. Otherwise stated, the hadronic shower will also cool down to sub-100 GeV energies. But as the disk density is a function of the position in the orbit before and after periastron passage, there are orbital configurations prone to the emission of both high-energy photons and neutrinos.

To simplify the discussion and get a numerical example of the processes involved, we set the half-thickness of the disk to a constant ($h \sim 3.5 \times 10^6$ cm) and consider an orbital configuration for which $L_{37} \sim 0.2$ before or after periastron passage. The cross section for pp interactions is $\sim$50 mb (Battiston et al. 1982). The probability for a pp interaction to take place within the disk is $1 - e^{-2h/\lambda_p} \gg 99\%$, where λ_p is the mean free path of the relativistic protons. It is worthwhile to point out that even though the photon and particle densities are similar, the $p\gamma$ cross section is 2 orders of magnitude smaller than the pp cross section.

On the other hand, the pion mean free path in this configuration is $\lambda_\pi \sim 10^6$ cm, which implies a charged pion survival probability (to its decay distance) of $P \approx e^{-\Gamma\, c\, \tau_\pi/\lambda_\pi}$, where τ_π is the $\pi^\pm$ lifetime, and Γ is its Lorentz factor. Then the probability for producing ν's of energy, 200 GeV and 400 GeV is, on average, 10% and 1%, respectively. We expect a rapidly fading signal of neutrinos with energies greater than 1 TeV.

There appears to be enough room for the disk density (or grammage) to acquire values such that all protons will partake in hadronic interactions, whereas some of the pions produced will decay to high-energy neutrinos at a level significant enough to show up in neutrino telescopes. To analyze this in detail, numerical simulations of a proton-induced cascade unfolding within an accretion disk were performed.

4. NUMERICAL SIMULATIONS

The accretion disk itself is simulated as a cylindrical volume of thickness $2h$ and is filled with elemental hydrogen at a density $n = 4 \times 10^{19}$ cm^{-3}. A 400 TeV value is retained as the average energy of each proton in the beam even for $L_{37} \approx 0.2$ because the uncertainties in all other parameters involved dilute the deviation from the fiducial result. The generation and tracking of secondary particles in the cascade development was performed using GEANT4, a simulation tool kit designed for operation up to center-of-mass energies $s^{1/2} \sim 100$ GeV that provides general-purpose tools for the simulation of the passage of particles through matter (Agostinelli et al. 2002).[5] We process the initial hadronic collisions (with $s^{1/2} > 100$ GeV) using the event generator DPMJET-II (Ranft 1995). This program, based on the Gribov-Regge theory, describes soft particle interactions by the exchange of one or multiple pomerons. (The inelastic reactions are simulated by cutting pomerons into color strings that subsequently fragment into color neutral hadrons.) In the energy range of interest, $s^{1/2} \sim (10^2$–$10^3)$ GeV, the average energy fraction of the highest energy baryon in the simulated pN collisions is roughly 30%. Therefore, on average, after three collisions, the energy of the leading particle will be degraded down to $\sim$10 TeV. The secondary meson spectra from these three collisions are given in Figure 2. Additionally, for these center-of-mass energies, the soft baryon channel comprises two nucleons, each carrying (on average) 1% of the energy of the incoming proton. These secondary distributions, together with the leading particle (degraded in energy), were injected into the cylindrical volume representing the disk. The position of the first interaction was selected randomly following a Poisson distribution with a mean equal to the proton mean free path. The second and third interaction points were selected with the same procedure, taking the preceding collision as a reference and going farther down within the disk. We then use the GEANT4 to track all particles. In this second step, all hadronic collisions are processed with GEANT4 implementation of GEISHA,[6] a program tuned to analyze experimental results of a variety of projectiles and targets in the few GeV energy range. A magnetic field of 6000 G threads the synthetic disk volume, whose direction is pointing upward in Figure 1. Variations in the B field across the disk do not affect the results presented below because most of the particles in the shower are produced in minimum bias events boosted in the forward direction (see Fig. 3).

One can see in Figure 4 the average number of ν's produced from pion decay per unit energy (bin size $\equiv \Delta E_\nu =$

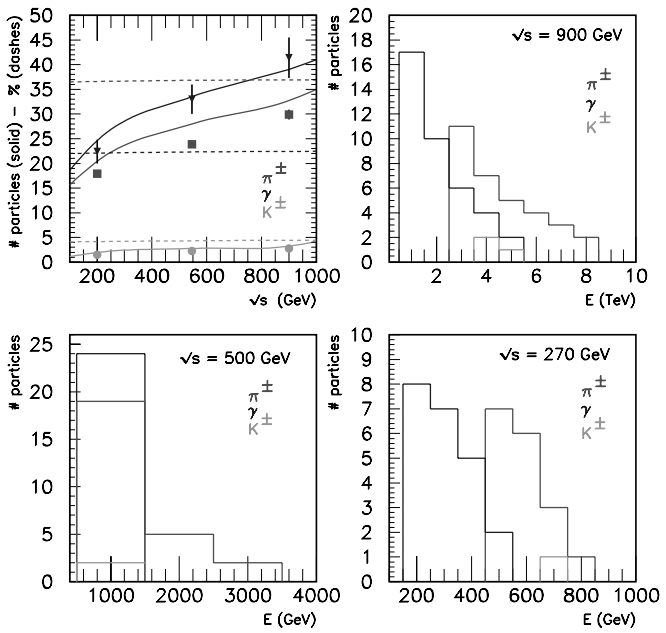

FIG. 2.—Characteristics of hadronic interactions implemented in the Monte Carlo event generator DPMJET–II. *Upper left panel*: Average multiplicities from pN collisions as a function of the center-of-mass energy (*solid lines*) together with the energy fraction (in percentages) going into secondary particles (*dashed lines*) from bottom to top, $K^\pm$, $\pi^\pm$, and γ. *Circles, squares, and triangles*: Average numbers of secondary particles produced in nondiffractive $p\bar{p}$ collisions measured by the UA5 Collaboration (Ansorge et al. 1989). The other three panels show the spectra of secondary particles produce in pN collisions at different center-of-mass energies. The spectrum of $K^{0L} + K^{0S}$ is roughly equal to that of $K^\pm$.

[5] Go to http://wwwinfo.cern.ch/asd/geant4/geant4.html for more information.

[6] H. Fesefeldt 1985, preprint (PITHA-85-02) and CERN divisional reports (CERN-DD-EE-81-1 and CERN-DD-EE-80-2).

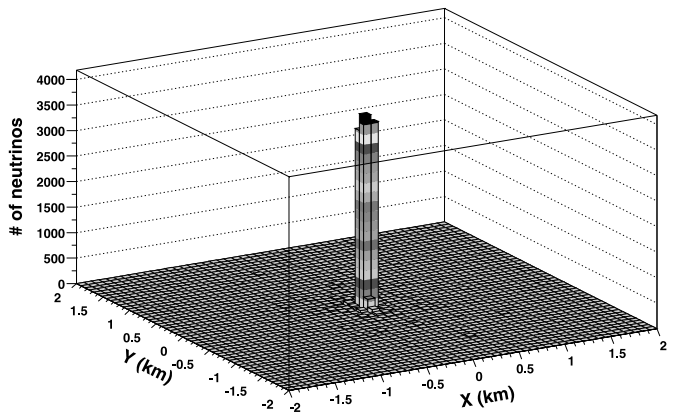

FIG. 3.—Neutrino lateral distribution from a proton shower in a typical accretion disk setting. The *x*-*y* plane is parallel to the disk. Because the secondary pions are produced with very low transverse momentum, most neutrinos are produced near the shower core.

50 GeV). The tail of the energy distribution is very well fitted by a power law, $A_0\ E_\nu^{-\gamma}$, with values of A_0 and γ given in the figure. *Therefore, a monoenergetic beam of high-energy protons impacting onto an accretion disk produces outgoing ν's with a power-law spectrum.*

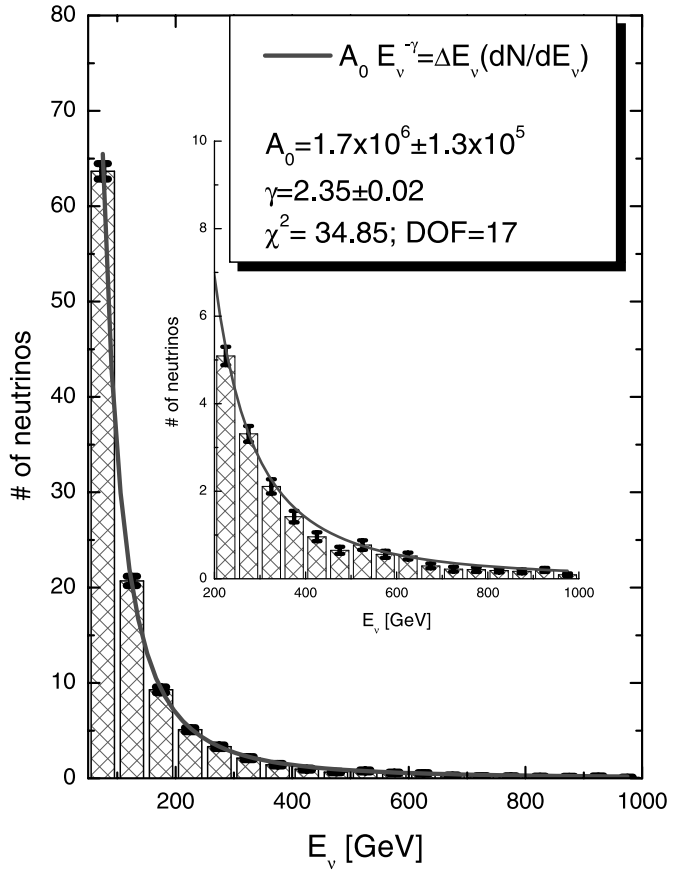

FIG. 4.—Neutrino energy distribution generated by pion decay induced by the collision of 400 TeV protons onto an accretion disk of a typical X-ray binary. *Error bars*: rms fluctuations for each of the mean values, represented by the height of each box in the histogram. The latter were obtained averaging over 100 showers. *Solid line*: Fit to this spectrum, whose parameters are shown in the insert. *Inset*: High-energy tail of the distribution, together with the same fit.

5. THE NEUTRINO SIGNAL

Having estimated the ν spectrum, we now analyze the S/N for a kilometer-scale detector like ICECUBE (Karle et al. 2002). This detector will consist of 4800 photomultipliers arranged on 80 strings placed at depths between 1400 and 2400 m under the South Pole ice. The strings will be located in a regular space grid covering a surface area of 1 km^2. Each string will have 60 optical modules (OM) spaced 17 m apart. The number of OMs that have seen at least one photon (generated by Čerenkov radiation produced by the muon that resulted from the interaction of the incoming ν in the Earth's crust) is called the channel multiplicity, $N_{\rm ch}$. The multiplicity threshold is set to $N_{\rm ch} = 5$, which corresponds to an energy threshold of 200 GeV (Alvarez-Muñiz & Halzen 2002). The angular resolution of ICECUBE will be 0°.7, which implies a search window of $\sim 1^\circ$ radius (Karle et al. 2002).

The event rate of the atmospheric ν background that will be detected in the search bin is given by

$$\left|\frac{dN}{dt}\right|_B = A_{\rm eff} \int dE_\nu \ \frac{d\Phi_{\rm B}}{dE_\nu}\ P_{\nu\to\mu}(E_\nu)\ \Delta\Omega_{1^\circ\times 1^\circ}\ , \qquad (4)$$

where $A_{\rm eff}$ is the effective area of the detector, $\Delta\Omega_{1^\circ\times 1^\circ} \approx 3\times 10^{-4}$ sr, and $d\Phi_B/dE_\nu \lesssim 0.2\ (E_\nu/{\rm GeV})^{-3.21}\ {\rm GeV}^{-1}\ {\rm cm}^{-2}\ {\rm s}^{-1}\ {\rm sr}^{-1}$ is the $\nu_\mu + \bar\nu_\mu$ atmospheric ν flux (Volkova 1980; Lipari 1993). Here $P_{\nu\to\mu}(E_\nu) \approx 3.3\times 10^{-13}\ (E_\nu/{\rm GeV})^{2.2}$ denotes the probability that a ν of energy $E_\nu \sim 1$–10^3 GeV, on a trajectory through the detector, produces a muon (Gaisser, Halzen, & Stanev 1995). On the other hand, the ν signal is

$$\left|\frac{dN}{dt}\right|_S = A_{\rm eff} \int dE_\nu \ \frac{d\Phi_{\nu_\mu}}{dE_\nu}\ P_{\nu\to\mu}(E_\nu)\ , \qquad (5)$$

where

$$\frac{d\Phi}{dE_\nu} = \left(\frac{\Delta\Omega}{4\ \pi}\right)^{-1} \frac{1}{4\ \pi\ d^2}\ \frac{d\Phi_0}{dE_\nu} \qquad (6)$$

is the incoming ν flux emitted by a source at a distance (d) from Earth with a beaming factor of $\Delta\Omega/4\pi$. Phenomenological estimates yield $\Delta\Omega/4\pi \sim 0.1$ (Cheng & Ruderman 1989). The ν emission spectrum is just $d\Phi_0/dE_\nu = N_p\ dN/dE_\nu$, where dN/dE_ν can be read from the first panel of Figure 4, and $N_p \approx 3\times 10^{33}$ is the total number of protons impacting the disk. It is noteworthy that the flux of neutrinos, which is dominantly $\nu_\mu + \bar\nu_\mu$ at production, is expected to be completely mixed in flavor upon arrival at Earth. Specifically, there is now strong evidence for maximal mixing among all neutrino species (Fukuda et al. 1998), which implies that the ν flux would be completely mixed after a propagation distance of (Bilenky, Giunti, & Grimus 1999)

$$L_{\rm osc} \approx 2.5\ \frac{E_\nu}{\rm GeV}\ \frac{{\rm eV}^2}{\Delta m_\nu^2}\ {\rm km}\ , \qquad (7)$$

where $\Delta m_\nu^2 \gtrsim 10^{-6}\ {\rm eV}^2$ is the ν-mass splitting. Putting all this together, we obtain

$$\frac{d\Phi_{\nu_\mu}}{dE_\nu} \approx \frac{1}{3}\frac{d\Phi}{dE_\nu}\ . \qquad (8)$$

A0535+26 is very close to Earth, only $\sim$2.6 kpc distant (Giovannelli & Sabau Graziati 1992). In addition, as only ν's going through the Earth can be identified, the northern

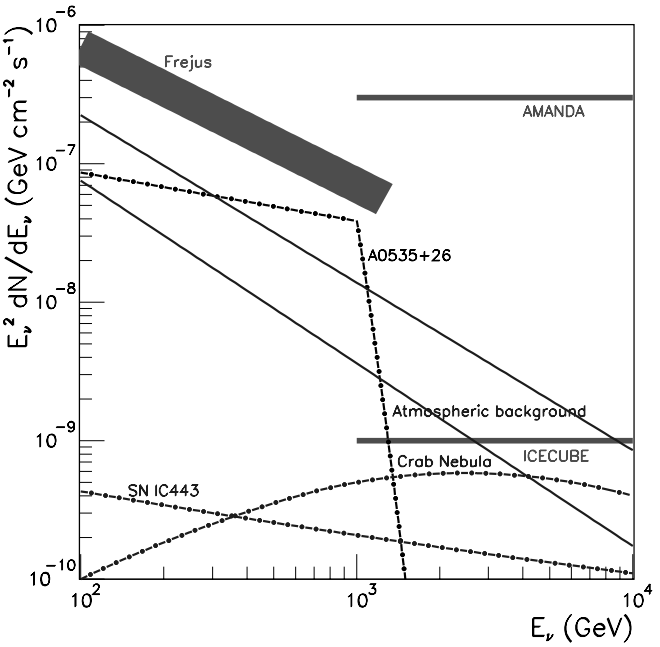

FIG. 5.—*Upper decreasing dash-dotted curve*: Expected $\nu_\mu + \bar{\nu}_\mu$ flux coming from A0535+26 with sharp cutoff above 1 TeV. The flux above this energy is subject to large uncertainties because of shower-to-shower fluctuations, and it is not being taken into account to compute the S/N, which is based only in the interval (300 GeV, 1 TeV). The shape of the cutoff given in this figure corresponds to that estimated using the phenomenological arguments about pion survival probability discussed in the main text. The atmospheric $\nu_\mu + \bar{\nu}_\mu$ background within a $1^\circ \times 1^\circ$ square of the source (*diagonal solid lines*), which corresponds to horizontal and vertical (*upper curve*) impacts (Volkova 1980; Lipari 1993). Also shown is the current upper limit on $\nu_\mu + \bar{\nu}_\mu$ flux for a source with differential energy spectrum $\propto E^{-2}$ and declination angle larger than 40° as reported by the AMANDA Collaboration (Ahrens et al. 2003) as well as the expected sensitivity of ICECUBE after its first 3 yr of operation (Hill et al. 2001). Assuming the flux is fairly uniform with decreasing angular bin, we scaled down to $\Delta\Omega_{2^\circ\times 2^\circ}$ (angular resolution of AMANDA) the current upper limit on diffuse $\nu_\mu + \bar{\nu}_\mu$ fluxes (90% CL) as reported by the Fréjus Collaboration (Rhode et al. 1996). We stress that the Fréjus detector was located in an underground laboratory in the Alps, and consequently, it had not a complete field of view of A0535+26. *Lower decreasing dash-dotted line*: $\nu_\mu + \bar{\nu}_\mu$ spectrum of SN IC 443 (Hill et al. 2001). This curve relies on the assumption that (on average) a pair of muon neutrinos with energy $E_\pi/4$ are produced in the pion-to-muon-to-electron decay chain of proton showers (in very low-density media) for every photon with energy $E_\pi/2$ (Gaisser, Protheroe, & Stanev 1998). *Bumpy curve*: One of the hypotheses (model II in Bednarek & Protheroe 1997) for $\nu_\mu + \bar{\nu}_\mu$ production in the Crab Nebula.

location of this source makes it accessible from the South Pole site of ICECUBE. Figure 5 illustrates the expected ν flux from A0535+26. The atmospheric ν background for a $1^\circ \times 1^\circ$ bin is indicated by the diagonal lines. Also indicated in the figure are the fluxes of several other point sources. It is clear that for 300 GeV $< E_\nu <$ 1 TeV, ν's coming from A0535+26 can dominate both over the background and over all other known sources. The S/N in the range $E_\nu \in (300\ \mathrm{GeV}, 1\ \mathrm{TeV})$, using equations (4) and (5) and considering an observing time of ~50 days, compatible with the period in which the accretion disk is forming or disappearing, is

$$S/N = \frac{N|_S}{\sqrt{N|_B}} \approx 1.7\ . \tag{9}$$

It is possible, then, that A0535+26 could be detected as a variable neutrino source even within the time span of one orbital period. The possibility of detection can be further improved by adding up several orbital periods, of which there are three per year. It is therefore possible that sources such as A0535+26 already could have been detected in the AMANDA data. In order to search for this possibility, two all-sky maps could be used[7] by (1) adding up all observations in periods where the source is expected to be ON, before and after periastron passage, and (2) adding up all observations with the source in OFF mode, at the periastron. The difference between these two maps, weighted by the respective integration times, should leave only one source on the sky, disregarding that this source in itself is well below the background for the experiment. Of course, the same technique can work for ICECUBE. A few years' integration time would add up tens of orbital revolutions, and detection of A0535+26 should be unambiguous. Indeed, A0535+26 is, in projection, less than 5° away from the Crab Nebula, which was suggested as a potential detection by AMANDA (Barwick et al. 2002). This detection is based on a $\sim 6^\circ \times 6^\circ$ binning of the northern hemisphere. It is not implausible, then, that A0535+26 may significantly contribute to this angular bin, particularly at energies below 1 TeV.

From a technical point of view, ICECUBE must select a soft energy cutoff to observe this source since A0535+26 shines mostly below 1 TeV. (The channel multiplicity threshold of the experiment must be set as $5 \le N_{\mathrm{ch}} \le 30$; Karle et al. 2002.) A next-generation observatory such as NEMO (Riccobene et al. 2002) would improve the angular resolution to ~0°.3, which would increase the S/N by a factor of 3.

6. CONCLUDING REMARKS

In summary, a wide range of parameters that describe the physical situation of accreting neutron stars make them a bona fide population of ν emitters with power-law spectra. In the particular of case of A0535+26, the $\nu_\mu + \bar{\nu}_\mu$ flux between 300 GeV and 1 TeV overwhelms those of all other point sources and is clearly above the atmospheric background in a $1^\circ \times 1^\circ$ angular bin.

The neutrino signal will be periodic in nature. The accumulated signal during the apoastron, where there is no disk formed, and periastron passages will always be at the noise level. On the contrary, the accumulated signal during time spans before and after the periastron passage will be, as we have shown, significantly different from noise level. A reasonable integration time for neutrinos would then secure high-confidence detections of the appearance and disappearance of the accretion disk ($\gtrsim 3$ yr to reach a 5 σ effect). Complementary information from high-energy photon astronomy in the X- and γ-ray domain will be essential to confirm the hadronic origin of the radiation in accreting neutron star systems as well as for the study of the formation and loss of accretion disks in eccentric binary systems.

We have benefitted from discussions with Haim Goldberg, Christopher Mauche, and Rodin Porrata. The research of L. A. A. and T. P. M. was supported by the U.S. National Science Foundation grant PHY-0140407.

[7] We thank Rodin Porrata (LLNL) for bringing this to our attention.

The work of D. F. T. was performed under the auspices of the U.S. Department of Energy by University of California Lawrence Livermore National Laboratory under contract W-7405-Eng-48. D. F. T. is Lawrence Fellow in Astrophysics. The research of G. E. R. is mainly supported by Fundación Antorchas, with additional contributions from the agencies CONICET (PIP 0430/98) and ANPCT (PICT 03-04881). He is a member of CONICET.

REFERENCES

Agostinelli, S., et al. 2002, SLAC-PUB-9350
Ahrens, J., et al. 2003, ApJ, 583, 1040
Alvarez-Muñiz, J., & Halzen, F. 1989, ApJ, 576, L33
Ansorge, R. E., et al. 1989, Nucl. Phys. B, 328, 36
Barwick, S. W., et al. 2002, SPIE, submitted (astro-ph/0211269)
Battiston, R., et al. 1982, Phys. Lett. B, 117, 126
Bednarek, W., & Protheroe, R. J. 1997, Phys. Rev. Lett., 79, 2616
Berezinsky, V. S., Bulanov, S. V., Dogiel, V. A., Ginzburg, V. L., & Ptuskin, V. S. 1990, Astrophysics of Cosmic Rays (Amsterdam: North-Holland)
Berezinsky, V. S., Castagnoli, C., & Galeotti, P. 1985, Nuovo Cimento C, 8, 185
Bethe, H. A., & Heitler, W. 1934, Proc. R. Soc. London A, 146, 83
Bilenky, S. M., Giunti, C., & Grimus, W. 1999, Prog. Part. Nucl. Phys., 43, 1
Carroll, A. S., et al. 1979, Phys. Lett. B, 80, 423
Cheng, K. S., & Ruderman, M. 1989, ApJ, 337, L77
———. 1991, ApJ, 373, 187
Cox, A. N. 2001, Astrophysical Quantities ed. R. E. Lingenfelter & R. E. Rothschild, (4th ed; New York: Springer), 213
Finger, M. H., Wilson, R. B., & Harmon, B. A. 1996, ApJ, 459, 288
Fukuda, Y., et al. 1998, Phys. Rev. Lett., 81, 1562
Gaisser, T. K., Halzen, F., & Stanev, T. 1995, Phys. Rep., 258, 173
Gaisser, T. K., Protheroe, R. J., & Stanev, T. 1998, ApJ, 492, 219
Gaisser, T. K., & Stanev, T. 1985, Phys. Rev. Lett., 54, 2265
Ghosh, P., & Lamb, F. K. 1979a, ApJ, 232, 259
———. 1979b, ApJ, 234, 296
Giovannelli, F., & Sabau Graziati, L. 1992, Space Sci. Rev., 59, 1
Hartman, R. C., et al. 1999, ApJS, 123, 79
Hill, G. C., et al. 2001, Proc. XXXV Recontres de Moriond, preprint (astro-ph/0106064)
Janot-Pacheco, E., Motch, C., & Mouchet, M. 1987, A&A, 177, 91
Karle, A. 2002, preprint (astro-ph/0209556)
Kolb, E. W., Turner, M. S., & Walker, T. P. 1985, Phys. Rev. D, 32, 1145
Lipari, P. 1993, Astropart. Phys., 1, 195
Ranft, J. 1995, Phys. Rev. D, 51, 64
Rhode, W., et al. 1996, Astropart. Phys., 4, 217
Riccobene, G. 2002, Hamburg DESY Proc., Methodical Aspects of Underwater/Ice Neutrino Telescopes, ed. R. Wischnewski (Hamburg: DESY), 61
Romero, G. E., Kaufman-Bernado, M. M., Combi, J. A., & Torres, D. F. 2001, A&A, 376, 599
Shapiro, S. L., & Teukolsky, S. A. 1983, Black Holes, White Dwarfs, and Neutron Stars (New York: Wiley)
Volkova, L. V. 1980, Soviet J. Nucl. Phys., 31, 784